

Constraint-Based Planning and Control for Safe, Semi-Autonomous Operation of Vehicles

Sterling J Anderson, Sisir B. Karumanchi, and Karl Iagnemma

Dept. of Mechanical Engineering
Massachusetts Institute of Technology
Cambridge, MA, USA
{ster | sisir | kdi} @mit.edu

Abstract—This paper presents a new approach to semi-autonomous vehicle hazard avoidance and stability control, based on the design and selective enforcement of constraints. This differs from traditional approaches that rely on the planning and tracking of paths. This emphasis on constraints facilitates “minimally-invasive” control for human-machine systems; instead of forcing a human operator to follow an automation-determined path, the constraint-based approach identifies safe homotopies, and allows the operator to navigate freely within them, introducing control action only as necessary to ensure that the vehicle does not violate safety constraints. The method evaluates candidate homotopies based on “restrictiveness”, rather than traditional measures of path goodness, and designs and enforces requisite constraints on the human’s control commands to ensure that the vehicle never leaves the controllable subset of a desired homotopy. Identification of these homotopic classes in off-road environments is performed using geometric constructs. The goodness of competing homotopies and their associated constraints is then characterized using geometric heuristics. Finally, input limits satisfying homotopy and vehicle dynamic constraints are enforced using threat-based feedback mechanisms to ensure that the vehicle avoids collisions and instability while preserving the human operator’s situational awareness and mental models. The methods developed in this work are shown in simulation and experimentally demonstrated in safe, high-speed teleoperation of an unmanned ground vehicle.

Keywords—*Semi-Autonomous control, shared adaptive control, planning, obstacle avoidance, unmanned ground vehicles, teleoperation, human-machine interaction*

I. INTRODUCTION

Humans make mistakes. When humans control dynamic systems, the rate and ramifications of those mistakes increase. Whether it occurs while driving a car, controlling industrial machinery, or teleoperating an unmanned vehicle, human error can lead to costly and often deadly consequences. In 2010, over 32,000 people were killed and another 2.2 million injured in motor vehicle accidents in the United States alone [1]. The U.S. military is also strongly affected by human error, with vehicle crashes representing the leading cause of non-hostile deaths in Operation Iraqi Freedom [2]. Even unmanned ground vehicles are susceptible, as operators must not only cope with the challenges inherent to the manned driving task, but must perform many of the same functions with a restricted field of view, limited depth perception, potentially disorienting

camera viewpoints, and significant time delays [3]. Remotely operating a ground vehicle under these conditions while monitoring the vehicle’s health status, the status of the mission/tasks, and the condition of the environment leads to high failure rates, with many of today’s UGV’s failing before having completed even one full shift [4].

Semi-autonomous control offers a unique opportunity to improve human performance through the exploitation of human-automation synergies. As originally published in 1951 [5] and widely discussed since, humans and automation are uniquely well suited to specific types of tasks [6]. Whereas automation excels at responding quickly and precisely to well-defined or repetitive control objectives, humans tend to make more mistakes as the frequency and complexity of the control task increase. Conversely, humans have the unique ability to detect and contextualize patterns and new information, reason inductively, and adapt to new modes of operation, whereas automation typically struggles at these tasks. The goal of semi-autonomy is to exploit synergies in the abilities of humans and automation to improve planning and control performance of the combined system and – where possible – the actors therein.

A. Previous Work

Research to date in vehicle control has left a significant gap between fully-autonomous planning and control frameworks, which neither account for nor provide an effective means of cooperating with the human operator, and driver assistance systems which are limited to local, one-dimensional support. While these classes of system are distinct in their intended outcomes, their inability to effectively share control with a human driver has its root in a common, basic building block: each relies on specific, planned paths.

In the context of autonomous control, many methods exist for planning this path. Common path planning tools include rapidly-exploring random trees [7], graph search methods [8], potential fields analysis [9], and neural optimization techniques [10]. Control laws routinely used to track these reference paths include PID schemes, linear-quadratic regulators, and nonlinear fuzzy controllers. While many variations of this planning-then-control approach have proven effective in autonomous implementations [11], their reliance on a specific reference path (which is in many cases arbitrary, non-intuitive, and over-restrictive to a human operator), and consequent inability to account for the

planning preferences and control inputs of a human operator make them ill-suited for human-in-the-loop or “semi-autonomous” control.

At the other end of the vehicle safety community, with an eye on nearer-term, industry-driven objectives, researchers have developed systems that assist the human operator in avoiding collisions and loss of stability. These “active safety systems” traditionally fall into one of two categories: *reactive safety systems*, such as antilock brakes, traction controllers, electronic stability controllers, and lane-assist approaches monitor the current state of the vehicle and apply low-level control actions to meet some safety-critical criteria [12]. *Predictive safety systems*, on the other hand, consider not only the current state of the ego vehicle, but also the predicted state evolution of the vehicle and environmental hazards. These systems then preemptively assist the driver in identifying, assessing the threat posed by, and in some cases avoiding an impending hazard. Recent work in predictive safety has resulted in systems that use audible warnings [13], haptic alerts [14] and steering torque overlays [15] to help the driver avoid collisions [16], instability [17], or lane departure [18]. Similar to autonomous systems, the path-based prediction metrics used by these systems limits their ability to provide more than local, one-dimensional support.

Between the strategic, multidimensional capabilities of autonomous planning and control systems and the more tactical, one-dimensional focus of driver-assistance systems lies a significant need for truly semi-autonomous navigation; planning and control techniques capable of both strategic planning and intuitive, “intention-preserving” control support. We posit that such a system should be designed to accommodate the field-based planning and control technique humans have long been shown to exhibit [19]. Rather than obsessively planning and tracking a single path, humans tend instead to identify a field of safe travel – one that contains an infinite number of continuously deformable (“homotopic”) paths – and control the vehicle within it. This homotopy selection arguably represents the highest level of human reasoning employed in the navigation task and reduces the subsequent burden of calculating and applying appropriate control inputs to that of simply remaining within the desired homotopy. On an open roadway, for example, the preferred homotopy often contains many acceptable paths traversing a desired lane. In off-road environments, the desired homotopy may not be as clearly delineated, though vehicle dynamic constraints require that it exclude any region through which the vehicle cannot travel without colliding with obstacle(s). Figure 1 illustrates three prominent homotopies in a cluttered environment as they might be perceived by a human operator.



Figure 1. Visualization of prominent homotopies available to a human operator (image best viewed in color).

Instead of planning a path and restricting the human operator to that path, we propose a constraint-based semi-autonomous system that strategically limits the range of available inputs to ensure that the operator retains as much control freedom as possible without risking collision with obstacles or dynamic instability.

B. Paper Outline

This paper introduces a new approach to semi-autonomous control; one in which homotopies and their associated constraints are identified, characterized, planned, and enforced to ensure that the controlled system (an off-road ground vehicle in this case) avoids hazards and loss of stability without unduly restricting the control freedom of a human operator. Section II describes the methods used to plan and characterize constraints on the vehicle position. Section III then describes one method for converting those constraints into semi-autonomously enforceable constraints on the operator’s control commands. These methods are demonstrated in simulated control of a ground vehicle through an obstacle field (Section IV) and semi-autonomous teleoperation of a Kawasaki Mule through a similar field (Section V). The paper then closes with general conclusions.

II. CONSTRAINT PLANNING

Similar to its path-based counterpart, planning in constraint or “homotopy space” requires the identification of homotopies and an evaluation of their goodness. However, because the constraints bounding a path homotopy admit an infinite number of paths, identifying and evaluating the “goodness” of these constraints requires a new set of evaluation criterion from those commonly used in path planning. Whereas the goodness or “optimality” of a specific path is well-defined using metrics such as length, curvature, robustness, and dynamic feasibility, corresponding measures lose their traditional meaning when applied to a set of constraints and the many paths they admit. Further, planning methods typically used to design paths, such as grid-based search, potential fields, and sampling-based algorithms, will not necessarily work to plan constraints since the latter must be designed to circumscribe – rather than simply remain within – a safe operating region. In light of this inherent difficulty, a method is presented here based on the Constrained Delaunay Triangulation, which provides a useful physical boundary to, and heuristic evaluation of the many distinct paths existing within a given homotopy.

A. Homotopy Identification

As illustrated in Figure 1, any environment bifurcated by obstacles or impassible regions admits multiple path homotopies. A path homotopy is a set of paths that can be continuously deformed into one another without crossing infeasible regions. If a particular homotopy can be identified, vehicle position constraints may be designed at its edges to circumscribe the set of paths it contains and thereby ensure that the vehicle remains safely within it (avoiding collisions with obstacles).

In this work, we identify homotopies by decomposing two-dimensional configuration space $\mathbf{C} \in \mathbf{R}^2$ into a complete set of constrained Delaunay Triangles. The dual graph of this triangulation provides a search space through

which homotopies may be planned. That is, any feasible homotopy containing the vehicle's current position \mathbf{X}_0 , and the position of the goal location, \mathbf{X}_G , may be defined as a sequence \mathbf{H}^n of adjacent triangles $\mathbf{T}_0 \dots \mathbf{T}_n$ extending from the triangle circumscribing the vehicle's current position (\mathbf{T}_0 in Figure 2) to that containing the goal location(s). This goal may be described by a single point or by a given region of \mathbf{R}^2 , such as the distal edge of the local sensing window illustrated in red in Figure 2.

B. Homotopy Evaluation

In order to plan a set of constraints circumscribing a desired homotopy, metrics describing homotopy goodness must be defined and ascribed to individual triangles and transitions between them. We here propose two distinct heuristics for evaluating homotopy goodness: an estimate of the average "distance" traveled by paths within it, and an estimate of the control freedom available to an operator within a homotopy.

In this formulation, any path belonging to a particular homotopy $\mathbf{H}^n = \mathbf{T}_0 \cup \mathbf{T}_1 \cup \dots \cup \mathbf{T}_n$ will pass through each triangle \mathbf{T}_k in \mathbf{H}^n , where $k=1 \dots n$. A path enters \mathbf{T}_k through the edge it shares with \mathbf{T}_{k-1} ($\mathbf{E}_{k-1,k}$) and exits through $\mathbf{E}_{k,k+1}$ into \mathbf{T}_{k+1} . Thus, the average "distance" traveled by all triangle-monotonic (passing through each edge at most once) paths belonging to a given homotopy as it crosses \mathbf{T}_k may be heuristically described as the distance from the midpoint of $\mathbf{E}_{k-1,k}$ to that of $\mathbf{E}_{k,k+1}$. As Figure 2 illustrates, the dual graph embodying this heuristic closely resembles the Generalized Voronoi Diagram (GVD).

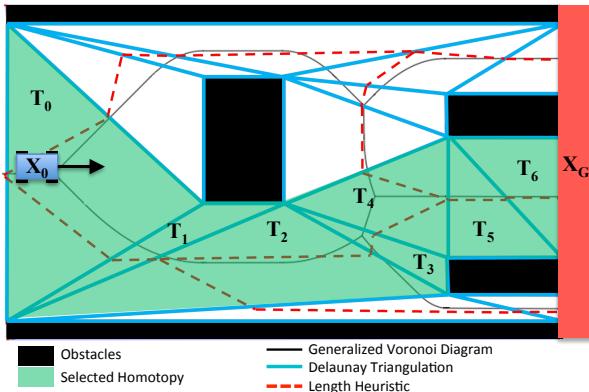


Figure 2. Illustration of triangulated environment showing homotopy selection and dual graph for length heuristic

While the average "length" of paths belonging to a particular homotopy may be described by the distance metric above, the "restrictiveness" and dynamic feasibility of the constraints bounding this homotopy require heuristic evaluations of the range of motion and control freedom they admit. To incorporate these considerations into the constraint-planning problem, we observe the following:

1. The dynamic feasibility of any path followed by a vehicle with Dubins constraints and friction-limited tires may be characterized by the lateral acceleration it requires.

2. This lateral acceleration is directly proportional to the square of vehicle velocity and inversely proportional to the radius of curvature of the path it follows.
3. In any homotopy \mathbf{H}^n , the maximum radius of curvature of any of the constant-velocity paths belonging to \mathbf{H}^n is limited by the "width" w_k , or minimum pass-through clearance of the Delaunay Triangles comprising the homotopy. As illustrated in Figure 3, w_k is calculated as the perpendicular distance from the constrained edge of the triangle to the apex opposite the constrained edge. The blue dashed line in Figure 3 illustrates the maximal radius path belonging to this homotopy.
4. This maximal curvature is also affected by the relative orientation of adjacent constrained edges, or equivalently, the difference in orientation $\phi_{k-1,k}$ for adjacent line segments L_{k-1} and L_k of the dual graph used to calculate "length" (these being parallel to the constrained edge).

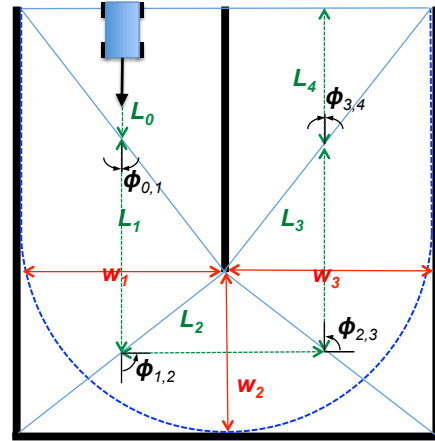


Figure 3. Illustration of a triangulated channel and the heuristics used to describe constraint restrictiveness and dynamic feasibility

With heuristics L_k , w_k , and ϕ_k thus calculated, a graph search (Dijkstra's algorithm is used here) may be performed to calculate the optimal path homotopy (a "channel" made of adjacent triangles) and its associated constraints. In the results shown in this paper, the objective function is defined as

$$\min_{T_i \dots T_n} \sum_{i=0}^n \left(k_L (L_{i-1,i}) + k_w \frac{1}{\min(w_{i-1}, w_i)} + k_\phi |\phi_{i-1,i}| \right) \quad (1)$$

$$\text{s.t. } \begin{aligned} X_G &\subseteq T_G \\ E_k &= \{(T_k, T_{k+1})\} \quad \text{where } E_k \text{ is unconstrained} \end{aligned} \quad (2)$$

This objective function incorporates an estimate of average homotopy "length" with an approximation of the control freedom and dynamic stability available to the vehicle as it traverses the homotopy.

III. CONSTRAINT ENFORCEMENT

In the previous section, an objective function was defined to assess the goodness of a given homotopy. Once a desired homotopy has been identified, vehicle position constraints circumscribing the homotopy must be converted into semi-

autonomously enforceable constraints on the human operator's control inputs as the vehicle traverses the constrained region.

To calculate these limits, a finite-horizon model predictive (MPC) controller is used to predict the vehicle state evolution within the desired homotopy under a stability-optimal control input sequence. The nearness of the predicted trajectory to stability limits is then used to compute the steering constraint applied at the vehicle and the torque feedback provided to the operator. These steps are briefly described below.

The MPC controller bases its predictions on a 4-wheeled vehicle model with slip and yaw dynamics. Defining vehicle states, outputs, inputs, and disturbances by \mathbf{x} , \mathbf{y} , \mathbf{u} , and \mathbf{v} , respectively, discrete plant dynamics are described by

$$\mathbf{x}_{k+1} = \mathbf{A}\mathbf{x}_k + \mathbf{B}_u\mathbf{u}_k + \mathbf{B}_v\mathbf{v}_k \quad (3)$$

$$\mathbf{y}_k = \mathbf{C}\mathbf{x}_k + \mathbf{D}_v\mathbf{v}_k \quad (4)$$

A quadratic objective function over a prediction horizon of p sampling intervals is defined as

$$J_k = \sum_{i=k+1}^{k+p} \frac{1}{2} \mathbf{y}_i^T \mathbf{R}_y \mathbf{y}_i + \sum_{i=k}^{k+p-1} \frac{1}{2} \mathbf{u}_i^T \mathbf{R}_u \mathbf{u}_i + \sum_{i=k}^{k+p-1} \frac{1}{2} \Delta \mathbf{u}_i^T \mathbf{R}_{\Delta u} \Delta \mathbf{u}_i + \frac{1}{2} \rho_\varepsilon \varepsilon^2 \quad (5)$$

where \mathbf{R}_y , \mathbf{R}_u , and $\mathbf{R}_{\Delta u}$ represent diagonal weighting matrices penalizing deviations from $\mathbf{y}_i = \mathbf{u}_i = \Delta \mathbf{u}_i = \mathbf{0}$, ρ_ε represents the penalty on constraint violations, n denotes the number of free control moves, and ε represents the maximum constraint violation over the prediction horizon p . Inequality constraints on vehicle position (\mathbf{y}), inputs (\mathbf{u}), and input rates ($\Delta \mathbf{u}$) are then defined as:

$$\begin{aligned} \mathbf{y}^j_{\min}(i) - \varepsilon \mathbf{V}^j_{\min}(i) &\leq \mathbf{y}^j(k+i+1|k) \leq \mathbf{y}^j_{\max}(i) + \varepsilon \mathbf{V}^j_{\max}(i) \\ \mathbf{u}^j_{\min}(i) &\leq \mathbf{u}^j(k+i+1|k) \leq \mathbf{u}^j_{\max}(i) \\ \Delta \mathbf{u}^j_{\min}(i) &\leq \Delta \mathbf{u}^j(k+i+1|k) \leq \Delta \mathbf{u}^j_{\max}(i) \end{aligned} \quad (6)$$

$$\begin{aligned} i &= 0, \dots, p-1 \\ \varepsilon &\geq 0 \end{aligned}$$

where the vector $\Delta \mathbf{u}$ represents the change in input from one sampling instant to the next, the superscript “ $(\bullet)^j$ ” represents the j^{th} component of a vector, k represents the current time, and the notation $(\bullet)^j(k+i|k)$ denotes the value predicted for time $k+i$ based on the information available at time k . The vector \mathbf{V} allows for variable constraint softening over the prediction horizon, p , when ε is included in the objective function. The vectors \mathbf{y}^j_{\min} and \mathbf{y}^j_{\max} are sampled from the edges of the constrained channel \mathbf{H}^n . Also note that input constraints enforced in the MPC calculation are simply those imposed by available actuation.

The state trajectory $\bar{\mathbf{x}}$ predicted by the MPC solution represents the state evolution of maximum stability that can be achieved given the vehicle's current position, dynamics, and homotopy constraints (imposed by \mathbf{H}^n). As such, the nearness of this prediction's stability-critical states to their physical limits provides a useful indication of the need for intervention and a natural boundary for the current vehicle input. Here, we define by “threat”, Φ , the maximum predicted value of a stability-critical state (front wheel

sideslip in this case). We then adjust the steering command seen by the vehicle to

$$u_{\text{vehicle}} = K(\Phi)u_{\text{MPC}} + (1 - K(\Phi))u_{\text{driver}}, \quad (7)$$

where $K \in [0 \ 1]$ is computed using a piecewise linear function which ensures that at low threat, the vehicle closely matches operator commands and at high threat – when the safest maneuver satisfying homotopy constraints approaches the limit of vehicle stability – the vehicle steering command tracks the optimal command predicted by the MPC controller. For a complete treatment of the threat assessment and the shared control method used in (7), the reader is referred to the authors' previous work in [20].

In addition to the constraint imposed on (or adjustment made to) the vehicle steering (which is transparent to the human operator), experimental tests also fed back a tactile set of “soft” constraints on the position of the steering wheel. This feedback provides a greater situational awareness to the human operator, particularly in teleoperation scenarios, as it indicates not only where the input constraints lie, but also how urgently they must be satisfied in order to avoid collision or loss of control. The resistance torque applied to the operator's steering wheel is calculated as

$$T = k_{\max} K |\delta_{\text{driver}} - \delta_{\text{MPC}}| \quad (8)$$

where k_{\max} represents the maximum available steering wheel torque and is used to re-dimensionalize K . Figure 4 illustrates the (hypothetical) response of the torque restoring function to increasingly threatening MPC predictions.

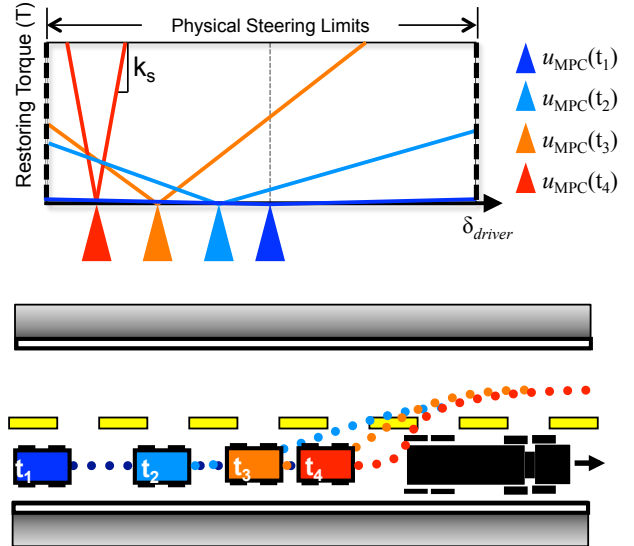


Figure 4. Scenario illustration showing the response of the restoring torque function as a vehicle successively approaches a hazard from behind

Notice that as time progresses (denoted by t_i labels on the host vehicle), the threat posed by the optimal maneuver prediction increases in severity. Additionally, the immediate steering command required to track this optimal trajectory begins to drift leftward. The combined effect of an increasingly-urgent, and progressively-leftward u_{MPC} recommendation increases k_s and shifts the torque resistance trough. In the limiting case for which only the optimal

steering command can reasonably be expected to avoid both the hazard and loss of control (sometime shortly after t_d), the controller exerts the maximum available torque on the operator's steering wheel, essentially ensuring that the operator not only cedes to the requirements of the controller, but is also aware of exactly what steering action is being taken by the vehicle.

IV. SIMULATION TESTING

The constraint-based semi-autonomous controller was simulated using a nonlinear ADAMS model of a generic light truck. The MPC controller ran at 20 Hz. Its prediction and control horizons were calculated over 60 and 40 timesteps, respectively. Parameters in the MPC model were configured to closely match those of the ADAMS plant, vehicle velocity was set at a constant 20 m/s, and simulated driver steering input was set to 0 degrees for generality. Figure 5 shows the path homotopy and associated position constraints designed by the path planner (green channel) as well as the control constraint imposed on the vehicle steering input (colorbar). Note that given the vehicle's initial position at (0,-2) [m], a shortest-path homotopy would have passed under the obstacles. Because this path is more tortuous and offers less control freedom to the human operator, the objective function described in (1) instead chooses the wider and less dynamically-challenging homotopy passing above the obstacles. Input constraints are initially large in order to avoid the impending hazard, but quickly relax as the vehicle enters a less restricted region of the homotopy above the obstacles. Finally, we note that the "ricochet" off the upper obstacle occurs because the simulated "human" input remains at zero for the entire maneuver. In practice, the significant control freedom offered by the relaxed constraints between $x=40$ and 80 meters allows the human operator to straighten out of desired.

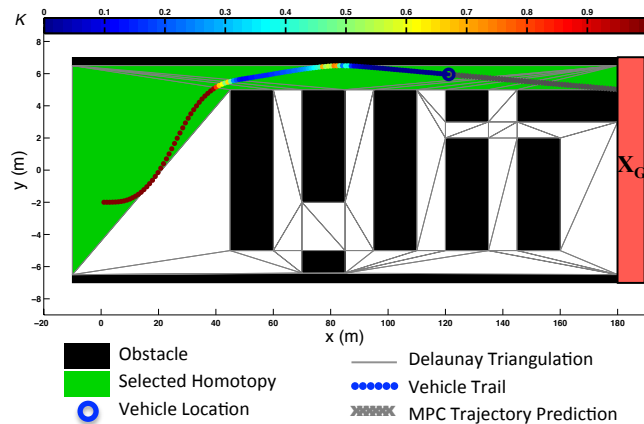


Figure 5. Simulation results demonstrating constraint-based semi-autonomous control through an obstacle field

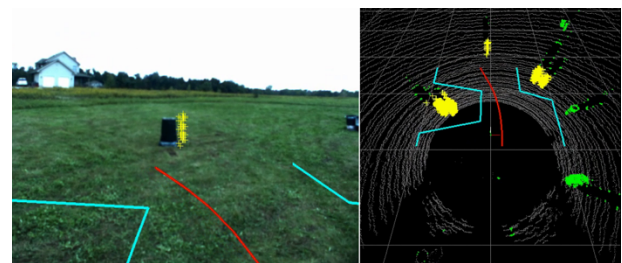
V. EXPERIMENTAL TESTING

Experimental testing was performed on a Kawasaki 4010 Mule fitted with steering and braking actuators, an omnidirectional video head, Velodyne LIDAR, NavCom GPS, and a triaxial IMU. An onboard Linux PC ran controller code and transmitted video and other data to a teleoperator control station over an 802.11g wireless link. At the remote control station, a teleoperator received video and

state feedback data on a computer monitor and issued steering commands through a Logitech G27 steering wheel. Torque constraints were applied to the steering wheel via its dual-motor force feedback mechanism capable of applying 0-3.1 N-m of torque in either direction. Barrels were arranged on an open field as obstacles and the teleoperator was instructed to navigate the vehicle from a start to a goal location without hitting them.



(a)



(b)

Figure 6. Experimental setup (a) and overlay of constraints (cyan) and MPC prediction (red) on video and LIDAR feed (b)

In order to simulate periodic loss of vision caused by random occurrences such as camera obfuscation, sensor outages, and loss of communication, the camera feed seen by the teleoperator was blanked at random intervals for up to 2 seconds at a time as he navigated the obstacle course at an average speed of 13 km/hr. A successful run was defined as one in which the vehicle crossed the obstacle field without colliding with any obstacles (verified by onboard safety personnel). Figure 7 shows the result of one of the ten experiments conducted with this configuration. In this run, control intervention from the semi-autonomous controller prevented the vehicle from colliding with obstacles when the driver's inputs were considered unsafe. Note that the drift observed in obstacle locations (and apparent overlap between obstacles and the vehicle path) is the result of a sub-par IMU.

In all, ten trials without any semi-autonomous assistance and ten trials with assistance were tested. Without assistance, the teleoperator collided with an obstacle 10 out of 10 times (0% success rate). With it, only 3 runs resulted in collision (70% success rate). This was achieved while maintaining an average constraint enforcement (K) value across all semi-autonomous runs of just 25% and an RMS steering wheel resistance torque of just 1.5 N-m. The three failures observed under semi-autonomous control were due to sensing limitations; in regions with high obstacle density, the 3m x 3m blind spot of the Velodyne sensor lost track of obstacles, resulting in constraints that did not preclude their position. When constraint positions were predicted and imposed in software (to simulate perfect sensing), collisions did not occur. It is expected that upgrading the inertial navigation

hardware will allow the sensing algorithm to maintain obstacle locations in a global frame and thereby avoid failures like these.

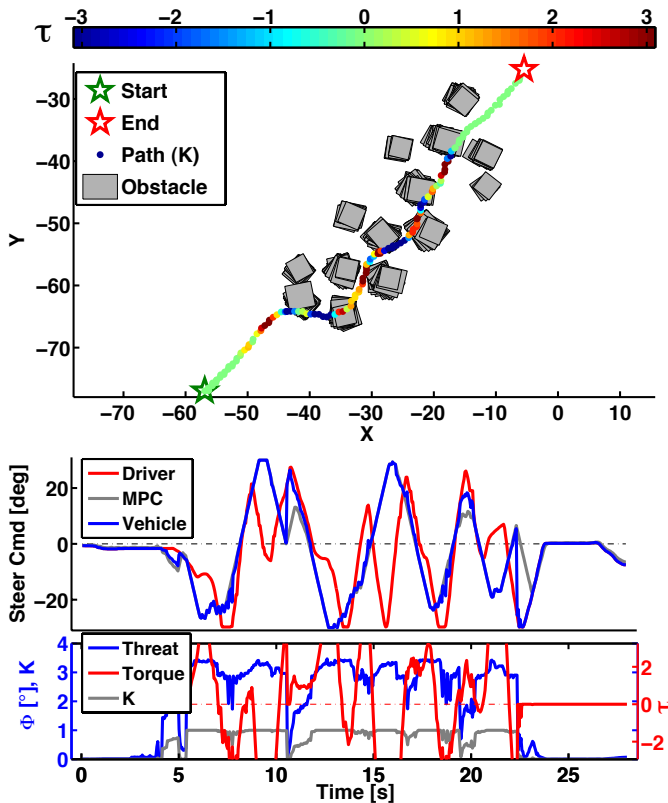


Figure 7. Data from an experimental run through an obstacle field

VI. CONCLUSIONS

Semi-autonomous navigation requires planning and control methods capable of identifying desirable path homotopies and ensuring that the controlled system remains within them. This paper has illustrated one method for achieving minimally-restrictive, homotopy-based control through the planning and enforcement of constraints – rather than reference paths – on the states and control inputs of the vehicle. This method has been shown in simulation and experiment to effectively assist a human driver in avoiding collisions while navigating a vehicle through an obstacle field. Finally, while the results shown here are promising, further work studying the feasibility and “goodness” of path homotopies and the effects of various input constraint enforcement techniques on the performance and situational awareness of human drivers remain to be conducted.

ACKNOWLEDGMENT

The authors would like to thank James Walker, Dan Rice, Kevin Melotti, Victor Perlin, Bryan Johnson, Rob Lupa, and Mitch Rohde for their assistance in setting up the Mule test vehicle and conducting experiments. This material is based on work supported by the US ARO under contract W911NF-11-1-0046 and DARPA DSO under the M3 program.

REFERENCES

- [1] National Highway Traffic Safety Administration (NHTSA), “2010 Motor Vehicle Crashes: Overview,” US Department of Transportation, Washington, D.C., Research Note DOT HS 811 552, Feb. 2012.
- [2] Defense Manpower Data Center, Statistical Information Analysis Division, “Military Casualty Information: Global War on Terrorism,” Data, Analysis, and Programs Division, Jan. 2012.
- [3] C. E. Lathan and M. Tracey, “The effects of operator spatial perception and sensory feedback on human-robot teleoperation performance,” *Presence*, vol. 11, no. 4, p. 368–77, 2002.
- [4] J. Carlson and R. R. Murphy, “How UGVs physically fail in the field,” *Robotics, IEEE Transactions on*, vol. 21, no. 3, pp. 423–437, 2005.
- [5] P. M. Fitts, M. S. Viteles, et al., “Human engineering for an effective air-navigation and traffic-control system, and appendixes 1 thru 3,” Mar. 1951.
- [6] T. B. Sheridan and R. Parasuraman, “Human-Automation Interaction,” *Reviews of Human Factors and Ergonomics*, vol. 1, no. 1, pp. 89–129, Jun. 2005.
- [7] J. Leonard, J. How, et al., “A perception-driven autonomous urban vehicle,” *Journal of Field Robotics*, vol. 25, no. 10, pp. 727–774, 2008.
- [8] R. Vaidyanathan, C. Hocaoglu, T. S. Prince, and R. D. Quinn, “Evolutionary path planning for autonomous air vehicles using multiresolution path representation,” in *Proc. of IROS 2001*, Maui, HI, United States, 2001, vol. 1, pp. 69–76.
- [9] E. J. Rossetter and J. Christian Gardes, “Lyapunov based performance guarantees for the potential field lane-keeping assistance system,” *Journal of Dynamic Systems, Measurement and Control, Transactions of the ASME*, vol. 128, no. 3, pp. 510–522, 2006.
- [10] Dong Kwon Cho and Myung Jin Chung, “Intelligent motion control strategy for a mobile robot in the presence of moving obstacles,” in *Proceedings IROS '91. IEEE/RSJ International Workshop on Intelligent Robots and Systems '91. Intelligence for Mech. Systems*, 3–5 Nov. 1991, New York, NY, USA, 1991, pp. 541–6.
- [11] Y. Kuwata, S. Karaman, J. Teo, E. Frazzoli, J. P. How, and G. Fiore, “Real-time motion planning with applications to autonomous urban driving,” *IEEE Transactions on Control Systems Technology*, vol. 17, no. 5, p. 1105–18, Sep. 2009.
- [12] Hai-bin Yu and Lu Gao, “Two-degree-of-freedom vehicle steering controllers design based on four-wheel-steering-by-wire,” *International Journal of Vehicle Autonomous Systems*, vol. 5, no. 1–2, pp. 47–78, 2007.
- [13] J. Jansson, “Collision avoidance theory with application to automotive collision mitigation,” Doctoral Dissertation, Linköping University, SE-581 83 LINKÖPING Sweden, 2005.
- [14] J. Pohl, W. Birk, and L. Westervall, “A driver-distraction-based lane-keeping assistance system,” *Proceedings of the Institution of Mechanical Engineers. Part I: Journal of Systems and Control Engineering*, vol. 221, no. 4, pp. 541–552, 2007.
- [15] R. Mobus and Z. Zomator, “Constrained optimal control for lateral vehicle guidance,” in *Proceedings of the 2005 IEEE Intelligent Vehicles Symposium, 6–8 June 2005*, Piscataway, NJ, USA, 2005, p. 429–34.
- [16] T. Pilutti, G. Ulsoy, and D. Hrovat, “Vehicle steering intervention through differential braking,” in *Proceedings of the 1995 American Control Conference, Jun 21–23 1995*, Seattle, WA, USA, 1995, vol. 3, pp. 1667–1671.
- [17] A. Alleyne, “A comparison of alternative obstacle avoidance strategies for vehicle control,” *Vehicle System Dynamics*, vol. 27, no. 5–6, p. 371–92, Jun. 1997.
- [18] T. Sattel and T. Brandt, “From robotics to automotive: Lane-keeping and collision avoidance based on elastic bands,” *Vehicle System Dynamics*, vol. 46, no. 7, pp. 597–619, Jul. 2008.
- [19] J. J. Gibson and L. E. Crooks, “A Theoretical Field-Analysis of Automobile-Driving,” *The American Journal of Psychology*, vol. 51, no. 3, pp. 453–471, Jul. 1938.
- [20] S. J. Anderson, S. C. Peters, T. E. Pilutti, and K. Iagnemma, “An Optimal-Control-Based Framework for Trajectory Planning, Threat Assessment, and Semi-Autonomous Control of Passenger Vehicles in Hazard Avoidance Scenarios,” *IJVAS*, vol. 8, no. 2–4, pp. 190–216, 2010.